Proc. Natl. Acad. Sci. USA
Vol. 94, pp. 2939–2944, April 1997
Biochemistry

Subunit arrangement in the human 20S proteasome

FRIEDRICH KOPP*, KLAVS B. HENDIL†, BURKHARDT DAHLMANN*‡, POUL KRISTENSEN†, AXEL SOBEK*, AND WOLFGANG UERKVITZ†

*Diabetes Forschungsinstitut, Auf'm Hennekamp 65, D-40225 Düsseldorf, Germany; and †August Krogh Institute, University of Copenhagen, Universitetsparken 13, DK-2100 Copenhagen Ø, Denmark

Communicated by Hans H. Ussing, University of Copenhagen, Copenhagen, Denmark, January 17, 1997 (received for review November 10, 1996)

ABSTRACT **In human 20S proteasomes two copies of each of seven different α-type and seven different β-type subunits are assembled to form a stack of four seven-membered rings, giving the general structure α_{1-7}, β_{1-7}, β_{1-7}, α_{1-7}. By means of immunoelectron microscopy and chemical crosslinking of neighboring subunits, we have determined the positions of the individual subunits in the proteasome. The topography shows that for the trypsin-like, the chymotrypsin-like, and the postglutamyl cleaving activities, the pairs of β type subunits, which are thought to form active sites, are nearest neighbors.**

The proteasome is a barrel-shaped proteinase particle found in eukaryotic cells and also in some archaea and eubacteria. It is responsible for the degradation of intracellular proteins, a process important for regulation of metabolism and cell division and, in higher animals, for immunological responses (1–3). The overall structure of proteasomes is well conserved during evolution and consists of four stacked rings. As most clearly shown for the proteasome from the archaeon *Thermoplasma acidophilum*, each of the two end rings consist of seven α subunits while each of the two central rings is composed of seven β subunits (4, 5). The active sites are formed by the N-terminal threonine residues of the β subunits, which face a central cavity in the cylindrical particle (6, 7).

Several distinct proteolytic activities have been detected in proteasomes from eukaryotic cells (8). Accordingly, 7 different types of β subunits have been detected in yeast cells and 10 in various mammalian cells (9). Analysis of yeast mutants defective in the chymotryptic or peptidylglutamyl peptide hydrolyzing (PGPH) activities of the proteasome has shown that in these cases mutations in two different β subunits were responsible for a single type of activity (10–13). Apparently, cooperation between two different β subunits is necessary for expression of a single activity and location of these subunits within the proteasome complex cannot be fortuitous. In mammals, interferon γ causes the replacement of certain β subunits by others, namely delta by LMP2, MB1 by LMP7 and Z by MECL1. Since mutual exchange takes place only within these pairs of β subunits, which harbor a free N-terminal threonine, but not between different pairs, each subunit may have a fixed position within the proteasome (14–17).

This holds true also for α-type proteasome subunits that during biogenesis act as a template for correct β subunit assembly (18, 19) and have also the function to bind regulatory complexes—e.g., PA28 and PA700 (20). These findings suggest that all subunits occupy defined positions in the eukaryotic proteasome. The aim of our investigations was to resolve the architecture of the human 20S proteasome by means of chemical crosslinking of neighboring subunits and by immunoelectron microscopy, a knowledge essential for the understanding of structure/function relationships of the eukaryotic proteasome.

MATERIALS AND METHODS

Purification of Proteasomes and Antibodies. Purification of 20S proteasomes from human placenta was performed as described (21). Preparation and characterization of mAbs is described in ref.s 22 and 23. Antibodies to HC5, HC7-I, and MB1 were produced in rabbits by immunizations with the peptides NMQNVEHVPLSLDRC, GYELSPTAAANFTRC, and DNVADLHEKYSGSTC, respectively, coupled to tuberculin "purified protein derivative" (24). The antibody specific for C8 was obtained as follows: subunits from human proteasomes were separated by two-dimensional PAGE, blotted onto nitrocellulose sheets, and stained with Ponceau S. Spots with C8 were excised, blocked with 2% polyvinylpyrrolidone-40 (Sigma), and incubated with 10% serum from a rabbit immunized with human intact proteasomes. The blots were then washed before the antibodies were released by incubation for 1 min in 0.2 M glycine/HCl, pH 2.1. The solution was neutralized, concentrated on a Mini Q PC 3.2/3 column (Pharmacia), and desalted on a PC 3.2/10 column (Pharmacia). The yield was about 0.7 μg.

Crosslinking of Proteasomes. Crosslinking was performed with cleavable crosslinkers as described (25–27). Purified proteasomes (500 μg) were mixed with 100 μM (final concentration) dithiobis(succinimidylpropionate) (DSP; Pierce) in a final volume of 1.25 ml 5 mM *N*-tris[hydroxymethyl]methyl-3-aminopropanesulfonic acid (TAPS; Sigma). The reaction mixture was incubated for 30 min at 0°C before addition of 250 μl of 125 mM lysine dissolved in 5 mM TAPS (pH 8.5) and further incubation for 45 min at 37°C and 16 h at 25°C for complete quenching. The enzyme solution was concentrated in a Microcon 10 (Amicon) and then mixed with an equal volume of Laemmli sample buffer. Alternatively, 500 μg of proteasomes were incubated for 30 min at 0°C with 150 μM (final concentration) ethyleneglycol bis(sulfosuccinimidyl-succinate) (sulfo-EGS; Pierce) in a final volume of 125 μl of 20 mM triethanolamine/HCl buffer (pH 7.0) before quenching with 25 μl of 125 mM lysine.

Isolation and Analysis of Crosslinked Subunits. Crosslinked subunits were separated and purified by one-dimensional SDS/PAGE on 13% acrylamide gels (28). Dimer bands were eluted from Coomassie stained gels or after Western blot analyses from nitrocellulose membranes. Alternatively, crosslinked subunits were isolated by two-dimensional PAGE. The crosslinked subunits were initially separated on 10–18% (wt/vol) SDS/PAGE gradient gels without slots and stained with Coomassie blue. Each band containing crosslinked subunits was excised separately and the protein eluted from the gel

The publication costs of this article were defrayed in part by page charge payment. This article must therefore be hereby marked "*advertisement*" in accordance with 18 U.S.C. §1734 solely to indicate this fact.

0027-8424/97/942939-6$2.00/0
PNAS is available online at **http://www.pnas.org**.

Abbreviations: PGPH, peptidylglutamyl peptide hydrolyzing; sulfo-EGS, ethyleneglycol bis(sulfosuccinimidyl-succinate); DSP, dithiobis(succinimidylpropionate).

‡To whom reprint requests should be addressed.

stripes (29). Proteins were then concentrated in a Microcon-10 concentrator to a volume of about 50 μl and the subunit dimers were further fractionated by two-dimensional PAGE as described by O'Farrell (30). The Coomassie-stained gel revealed multiple protein spots. Distinct bands or spots were excised. Cross-links formed with DSP were cleaved by incubation of gels with 100 mM dithioerythritol in 10% (wt/vol) mercaptoethanol for 16 h. Crosslinks obtained with sulfo-EGS were cleaved by incubation of gel pieces with 1 M hydroxylamine/HCl (pH 8.5) for 4 h. The gels were then washed in water and the monomers extracted by tumbling overnight at 37°C with 2 volumes of Laemmli sample buffer. The proteasome monomers obtained by cleavage of the crosslinkers were separated by SDS/PAGE and blotted onto nitrocellulose or polyvinylidene difluoride sheets. Total protein was detected with Aurodye (Amersham). Other lanes were used for identification of the monomers with subunit specific antibodies. Antibodies were detected either with tetramethylbenzine/H_2O_2, 5-bromo-4-chloro-3-indolyl phosphate/nitro blue tetrazolium, or with ECL chemiluminiscence detection system (Amersham).

Electron Microscopy. Conditions for formation of proteasome–antibody complexes and microscopical techniques have been described (21, 31).

RESULTS

Immunoelectron Microscopic Results. In the electron microscope, the eukaryotic 20S proteasome looks very similar to the *Thermoplasma* proteasome, but with respect to symmetry the two enzymes differ considerably in their quaternary structure (Fig. 1). Due to the defined arrangement of seven distinct kinds of α-type and seven β-type subunits, symmetry in the eukaryotic proteasome is reduced. In place of the seven minor 2-fold axes characteristic for the point group symmetry 72 of the *Thermoplasma* proteasome (6), the human proteasome has been postulated to contain but a single main 2-fold axis (21, 32). The axis of the particle that is coincident with the rotational axis of its enveloping cylinder is reduced to trivial identity—i.e., only complete rotation of the cylinder-shaped proteasome particle about 360° leads to an aspect indistinguishable from the original one. Consequently, to solve the quaternary structure of eukaryotic proteasomes the position of each pair of proteasome subunit relative to each other has to be defined.

Recently, epitope mapping by use of electron microscopic techniques has allowed us to localize the pair of β subunits N3 in the inner two rings (one subunit per ring) and, similarly, pairs of α subunits, C2 and XAPC7, in the end rings of the human placenta 20S proteasome (21, 31). As shown in Fig. 2*A*, pairs of antibodies to the α subunit C3 also bind in a defined spatial arrangement to each of the two terminal rings of the proteasome particle, confirming again that these rings consist

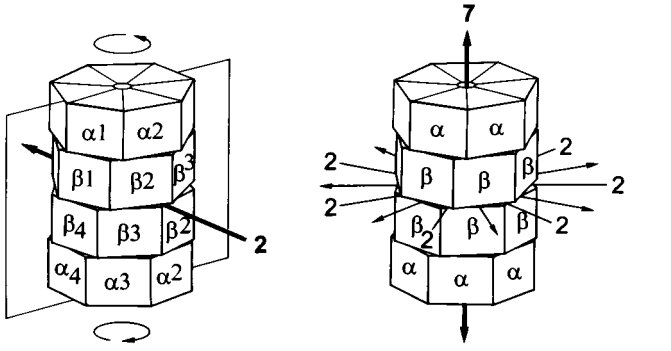

FIG. 1. Comparison of the general architecture of proteasomes from *T. acidophilum* and eukaryotes. Subunits in the eukaryotic (*Left*) and archaebacterial (*Right*) proteasomes are figured schematically by wedge-shaped bodies. The eukaryotic proteasome is a complex dimer (21) composed of seven different α subunits and seven different β subunits arranged in a counterrotated way with regard to the two halves of the particle, as indicated by their numbering and by circular arrows. The polar 2-fold axis of symmetry is indicated by the bold arrow, and the plane perpendicular to it cuts the particle into two halves of different composition, a feature significant for the construction of the subunit arrangement. The *Thermoplasma* proteasome is composed of two types of subunits, called α and β. The particle has a main 7-fold axis (bold) and seven minor 2-fold axes of symmetry (6).

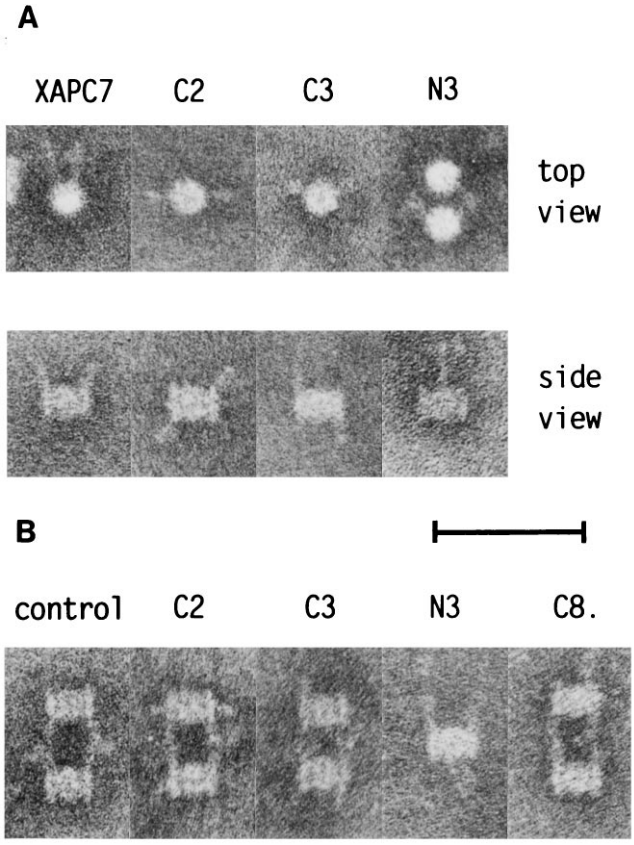

FIG. 2. Immunoelectron micrographs of human placenta 20S proteasome labeled with antibodies or their Fab fragments. (*A*) Epitope mapping on proteasomes with antibodies or Fab fragments specific for subunits XAPC7, C2, C3, and N3 either in top view (*Upper*) or in side view (*Lower*). Labeling reveals that all subunits occur pairwise. The arrangement of each kind of subunit pairs in the proteasome is characterized by a typical angle under which the corresponding epitopes appear in top views. The α-type subunits (XAPC7, C2, and C3) are located in the terminal rings as shown in the side views of the proteasomes labeled with Fab fragments, while the β-type subunit N3, labeled by complete antibody, is located in the central rings. (*B*) Double labeling of proteasomes with anti-XAPC7 as a first label and different subunit specific antibodies or Fab fragments as a second label. Antibodies specific for XAPC7 are known to form typical heterotetramers (21, 31), an example of which is shown (control). In these heterotetramers additional epitopes can be labeled and easily discriminated when Fab fragments are used as a second label as illustrated for C2 and C3. In the case of C8, whole antibody was used as a second label. In the case of N3/XAPC7, whole N3 antibody and Fab fragments of XAPC7 antibodies were used (see side view of XAPC7 in *A* as control). Subunits C3, C8, and N3 are located in the opposite half of the proteasome with respect to the pair of XAPC7 subunits. Graphic analysis of 23 side on configurations of proteasomes double labeled with XAPC7 antibodies and Fab fragments of C2 antibodies allowed us to locate the epitopes of C2 to the same half as XAPC7, since the angle between subunit C2 and the 2-fold axis amounts to 82.2° ± 12.4°. (The point of entrance of the 2-fold axis between the two XAPC7 subunits is defined as 0°; see Fig. 3*A*.) (Bar = 50 nm.)

Table 1. Position of epitopes in side view and angles between pairs of similar epitopes as seen in top view of the cylinder-shaped proteasome

Epitope pair	Sector angle measured between equal epitopes on top views		Closest $n \cdot 360°/7$	Epitope position in % of the normalized length	
	Mean ± SD	*N*		Mean ± SD	*N*
C2/C2	164.7° ± 18°	43	154.3°	9.6 ± 5	22
C3/C3	114.7° ± 6.9°	20	102.9°	13.1 ± 3.4	54
XAPC7/XAPC7	43.4° ± 8.3°	26	51.4°	10 ± 4	49
N3/N3*	103° ± 7.3°	14	102.9°	45.4 ± 2.5	35

N, number of measured cases.
*Data from ref. 31.

of α subunits. This finding also supports our conclusion that the human proteasome is a complex dimer with point group symmetry 2, which implies that a single copy of each of the seven different α and seven different β-type subunits is present in each half of the particle and occupies a defined position (Fig. 1). Thus, on profiles as well as on top views of the proteasome, identical subunits are always found in a symmetrical configuration with respect to the 2-fold axis (Fig. 2*A*). Therefore, we used the methodology described for localization of subunit N3 (31) to measure the sector angles between pairs of bound antibodies to C2, C3, and XAPC7. The results are summarized in Table 1. The bisectors coincide in end-on projection with the 2-fold axis. In addition, the mean distances of the binding sites of the three α-type subunits from the end planes of the supposed enveloping cylinder have been measured (21) (Table 1). To answer the question whether the subunits (epitopes) detected by labeling with the four different kinds of antibodies are located on the same or on the opposite half of the particle cylinder as defined by a central plane drawn perpendicular to the 2-fold axis (Fig. 1), we took advantage of our finding that the antibody specific for subunit XAPC7 forms characteristic heterotetrameric complexes consisting of two proteasomes linked to each other via two antibodies (21). In such a symmetric arrangement, in which the 2-fold axis is parallel to the image plane, both XAPC7 subunits are clearly located at the same side of the proteasome (Fig. 2*B*). Incubation of such heterotetrameric complexes with antibodies or their Fab fragments specific for C2, C3, and N3 resulted in double labeling of the proteasome particles with antibodies of different specificity. This technique allowed us to decide whether the subunits C2, C3, and N3 are located on the same or on the opposite side of the proteasome cylinder as the pair of XAPC7 subunits. As illustrated in Fig. 2*B*, the antibodies to C3 and to N3 bind to the half of the particle opposite to that containing the XAPC7 subunits. On the other hand, Fab fragments specific for subunit C2 bind to sites situated close to the central plane perpendicular to the 2-fold axis, a finding that is in line with the angle of 165° measured between two C2 subunits (Table 1). Statistical measurements allowed us to locate the epitopes of subunit C2 to the same half as XAPC7 (Figs. 2*B* and 3*A*). These data obtained on the four subunit-specific mAbs by immunoelectron microscopy clearly define the relative positions of the epitopes and therefore of four subunits within the proteasome. In similar experiments, complexes of proteasomes and antibody to XAPC7 were incubated with affinity purified rabbit antibody to the α subunit C8. The double-labeled proteasomes clearly showed that C8 is also found in the outer rings and in a position about opposite to XAPC7 (Fig. 2*B*).

Structural Framework Based on Immunoelectron Microcopic Results. Based on the results obtained by immunoelectron microscopy, a framework structure of the 20S proteasome was constructed as follows (Fig. 3). First, the two α-rings seem to be out of register since the angles of the sectors between

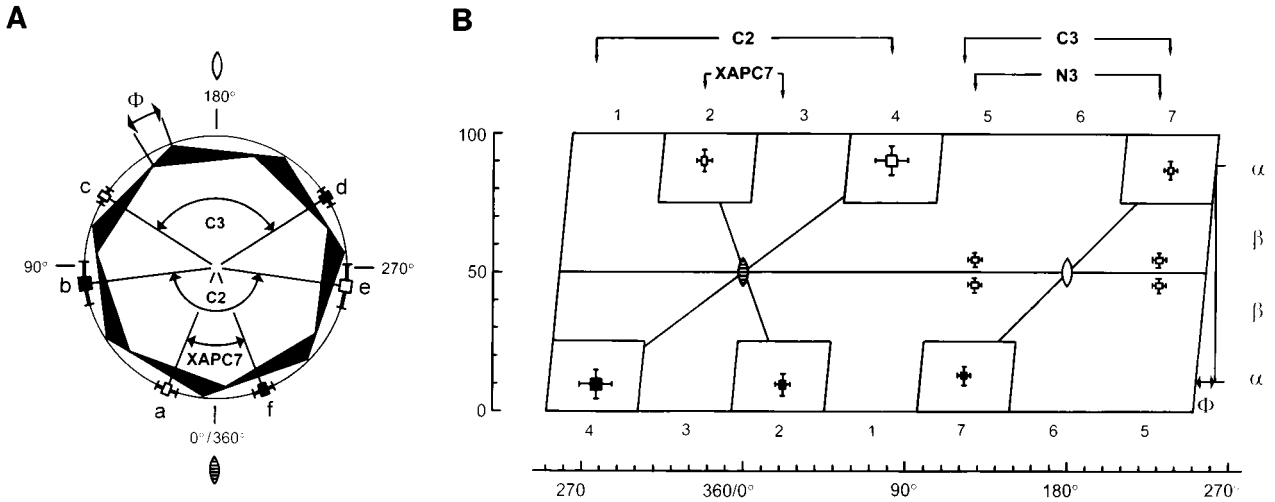

FIG. 3. Epitope arrangement as projected onto the cylinder envelope of the human proteasome. (*A*) End-on view showing schematically the positions of the three pairs of epitopes of α subunits C2, C3, and XAPC7 as obtained from angular measurements summarized in Tables 1 and 2. The epitope triplet a, c, e belongs to one α ring (white heptagon), the triplet b, d, f to the other α ring (black heptagon). The offset Φ of the two groups of epitopes amounts to 10°. The polar 2-fold axis of symmetry is indicated. (*B*) Rolled off cylinder envelope showing the epitope sites of the triplets (white and black) of α-type subunits C2, C3, and XAPC7 (*A*) as well as the two pairs of possible sites of epitopes of the β subunit N3. The standard deviations of the measurements of angular positions (abscissa) and those of the sites of epitopes with respect to the normalized length of the proteasome (ordinate) are indicated by crosses and SE (± 2) by the black and white squares. The offset Φ of 10° between the two triplets of epitopes as well as the points of entrance and exit of the 2-fold axis of symmetry (21) are indicated. The subunit positions fixed by electron microscopic results are marked by boxes.

Table 2. Angles between epitopes

Subunit	Circumference		Angular distance from site a, degree
	Site	Angle, degree	
XAPC7	a	21.7	**0**
C2	b	82.4	60.7
C3	c	122.7	**101**
C3	d	237.3	215.6
C2	e	277.6	**255.9**
XAPC7	f	338.3	316.6

Angles between one XAPC7 epitope (a) and the other epitopes (b–f), respectively, were calculated on the basis that the point of penetration of the of 2-fold axis of symmetry situated between the two XAPC7 epitopes (23) is chosen arbitrarily as 0°/360°. Values in bold are close to two (102.8°) and five (257.1°) times 360°/7, respectively, suggesting that subunits in positions a, c, and e are located in one α-ring whereas subunits in positions b, d, and f are located on the other α-ring.

epitope pairs C2/C2, C3/C3, and XAPC7/XAPC7 deviate by 10.4°, 11.8°, and −8.0° from the closest one, two, or three seventh of 360° (Table 1). The mean absolute deviation amounts to 10.1°. Second, taking into account that the pairs of epitopes of XAPC7 and of C2 are situated in the same half of the cylinder and the pair of epitopes of C3 in the opposite half with respect to the central plane vertical to the 2-fold axis indicated in Fig. 1, we obtain from measured sector angles a succession of epitopes (designated a–f) projected on the circumference of the proteasome cylinder as given in Table 2 and shown in Fig. 3*A*. Because only one triplet of C2, C3, and XAPC7 can be located together in one α-ring and the angles between the three subunits present within the same ring are expected to be close to one or a multiple of one-seventh of the complete circumference, we have calculated the sector angles between one XAPC7 epitope and the other epitopes. As shown in Table 2, only two angles in each case are very close to two- (102.8°) or five-seventh (257.1°) of a full circle. Thus, we conclude that the triplet a, c, e is situated in one α-ring, while the triplet b, d, f is located in the other α-ring (Fig. 3*A*).

Since we have, at the moment, data for only one β-type subunit, we cannot perform a similar discussion of the organization of the inner rings. It is, however, noticeable that subunit N3 is also well placed in the center of one-seventh (either position β_5 or β_7 in Fig. 3*B*) if a regular pitch within the 10° displacement is assumed between the two rings of β subunits (31).

The positions of the corresponding epitopes are mapped in both the top view of the cylinder and the rolled off side view of the cylinder (Fig. 3*B*). As can be seen in the drawings, there is room for one subunit between XAPC7 and C3, for another one between XAPC7 and C2 and for two subunits between C2 and C3. These sites are available for the four α subunits zeta, iota, C8, and C9, the positions of which, as well as those of the β subunits, were determined by nearest neighbor analysis using chemical crosslinkers.

Identification of Neighboring Subunits by Chemical Crosslinking. Neighboring proteasome subunits were crosslinked with cleavable reagents. The conditions were optimized to ensure a reasonable yield of crosslinked subunits while avoiding the formation of crosslinks between individual proteasome particles. Absence of the latter was checked by gel filtration and nondenaturing PAGE. Using the conditions specified in *Materials and Methods*, the crosslinking never exceeded 10% of total protein (results not shown).

Semipreparative SDS/PAGE was used to separate crosslinked from noncrosslinked proteasome subunits. As shown in Fig. 4*A*, subunits participating in crosslinking could be identified by immunoblotting with subunit specific antibodies. Because each band might contain more than one type of dimer, bands from such Coomassie-stained gels were excised

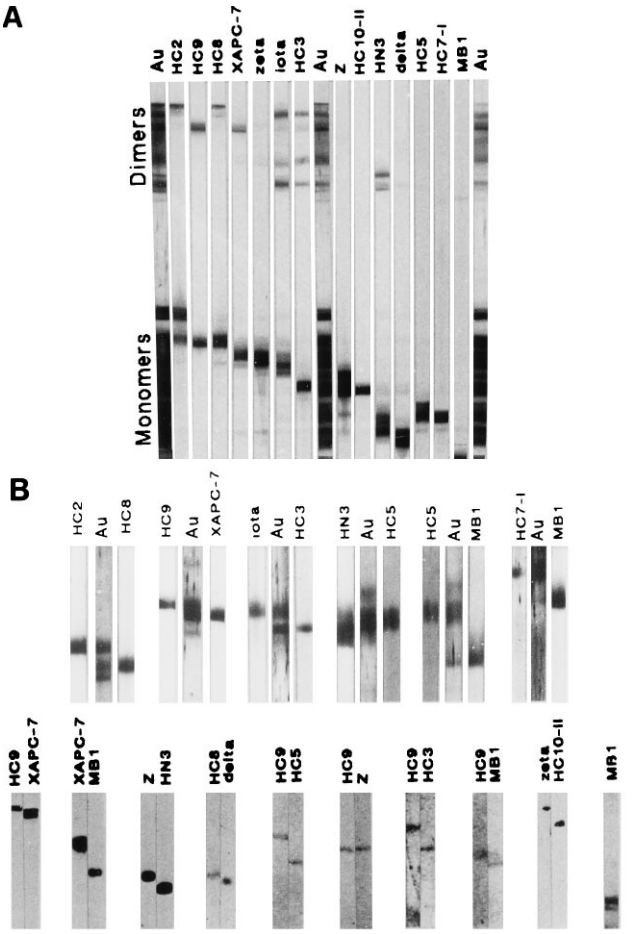

FIG. 4. Separation and analysis of crosslinked proteasome subunit pairs. (*A*) Separation of crosslinked proteasome subunit pairs. Proteasomes were crosslinked with sulfo-EGS and analyzed by SDS/PAGE and immunoblotting. Lanes Au were stained for total protein with colloidal gold (Aurodye; Amersham). Other lanes were incubated with subunit specific antibodies as indicated. (*B*) Individual subunit dimers were excised from one- or two-dimensional gels and the crosslinkers cleaved. The subunits from the dimers were then identified by a new round of SDS/PAGE and immunoblotting with all 14 subunit-specific antibodies. The subunits from individual crosslinked dimers are shown pairwise. For each dimer the remaining 12 antibodies showed no specific reaction. For dimers isolated only from one-dimensional PAGE, the lanes marked Au shows parallel lanes stained for total protein with colloidal gold to prove absence of other subunits.

and the crosslinker cleaved. The resulting free subunits were analyzed by SDS/PAGE. For several dimer bands, only two free subunits were formed, as detected by protein staining of blots, and these subunits could then be identified by immunoblotting. However, several bands in the dimer region of gels like that in Fig. 4*A* contained more than one type of dimer. Protein from such bands were eluted and separated by two-dimensional PAGE before the participating monomers were identified by protein staining and immunoblotting of SDS/PAGE gels. The results are summarized in Fig. 4*B*.

Arrangement of All Proteasome Subunits. For construction of the subunit arrangement within the proteasome, we presume that the α-type subunits are found exclusively in the outer rings whereas the central rings consist of β-type subunits analogous to the *Thermoplasma* proteasome. This is also in accordance with our microscopic data for four α subunits and one β subunit. Additionally, one has to take into account the 2-fold rotational symmetry of the particle when determining the positions of the different subunits as summarized in Fig. 5.

The α-type subunits C2, C3, and XAPC7 were localized by electron microscopy (Fig. 3*B*). The α-type subunit C9 is in

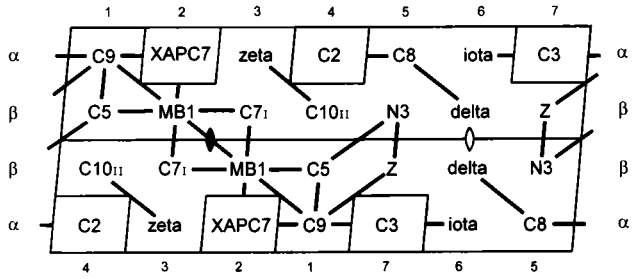

FIG. 5. The diagram presents the rolled-off cylinder, with positions in the α- and β-rings numbered as in Fig. 3*B*. The position of the boxed subunits are those identified by immunoelectron microscopy (Fig. 3*B*). The other subunits indicated were positioned by chemical crosslinking (solid lines) as shown in Fig. 4.

contact with both C3 and XAPC7 (Fig. 4) and must therefore be situated between them in position α_1. The crosslinked dimer iota-C3 places the α subunit iota in position α_6. Because C2 and C8 are also crosslinked, C8 must be in either the α_3 or the α_5 position. Immunoelectron microscopy showed that C8 is found about opposite to XAPC7 (Fig. 2*B*). This is compatible with C8 being in position α_5 but not in position α_3. Position α_3 must then be occupied by the last α type subunit, zeta. The arrangement of α subunits in the outer rings is therefore completed, as shown in Fig. 5.

Since subunits Z, C5, and MB1 all form crosslinks to C9, they must be neighbors in the same β-ring and occupy the positions β_1, β_2, and β_7. Thus, position β_7 cannot be occupied by subunit N3, a point which could not be decided by our immunoelectron microscopic studies (Fig. 3*B*). N3 must therefore be located in β_5. As N3 is also crosslinked to C5 and Z, the latter subunits must occupy the positions β_7 and β_1. Position β_2 must then be occupied by MB1, a conclusion corroborated by the dimer MB1–XAPC7 and in particular by MB1–MB1. C5 is a neighbor of MB1 (Fig. 4*B*) and is therefore in position β_1; so β_7 must be occupied by subunit Z.

Proteasome β subunits interact with β subunits in the adjacent ring via the H3 α-helices (6). Recently, it has been found that the effects of a mutation in the H3 α-helix of the yeast proteasome subunit PRE1 (yeast homologue of $C7_I$) can be suppressed by a mutation in the corresponding α-helix in PRE2 (yeast homologue of MB1), so $C7_I$ and MB1 must be in contact across the dyad axis of the proteasome (33). Since zeta and $C10_{II}$ are neighbors (Fig. 4*B*), $C10_{II}$ is in position β_4. Delta becomes crosslinked to C8 and must then be in position β_6 (Fig. 5). The assignments of these positions are corroborated by the dimer MB1–$C7_I$ (Fig. 4*B*) and two nonabundant dimers, MB1–$C10_{II}$ and N3–$C10_{II}$ (data not shown). The subunit topography is now complete, except for the handedness as discussed elsewhere (21).

DISCUSSION

Proteasomes from *Saccharomyces cerevisiae* mutated in the β subunits PRE1 ($C7_I$) and PRE2 [MB1, also called X or epsilon (34, 35)] exhibit considerably impaired chymotryptic activity without alterations of the PGPH and tryptic activities (10, 11). The N-terminal Thr residue of PRE2 (MB1) is thought to be part of the active site (6, 47). On the other hand, PRE1 ($C7_I$) has no such N-terminal Thr but appears to cooperate with PRE2 (MB1) to form the active site (10, 11, 36, 37). It remains to be determined which of the neighboring MB1/$C7_I$ pairs form the centers for chymotryptic activity, that in the same β-ring or that spanning the plane between the adjacent β-rings.

Yeast mutants deficient in proteasomal PGPH activity are mutated in the genes PRE3 and PRE4, the yeast homologues of delta and N3, respectively (12, 13, 38). Delta has the structural features of enzymatically active subunits while N3 does not (7). Thus, again an enzymatically active subunit cooperates with an "inactive" subunit to form an active center. The proximity of delta and N3 (Fig. 5) is in keeping with these results.

Antibody MCP444 was found to inhibit both the PGPH activity and the tryptic activity. The antibody binds to subunit N3 at an epitope very close to the neighboring subunit of the adjacent β-ring, Z, so that it partly overlaps this subunit (21). It is therefore likely that the third "active" subunit, Z, participates in the formation of the tryptic activity center. This assumption is substantiated by the finding that a mutation in PUP1, the yeast homologue to Z, results in loss of the tryptic activity (W. Heinemeyer and D. H. Wolf, personal communication). Additionally, a PRE3 (delta) mutant was recently found to be impaired not only in PGPH activity, but also in the tryptic activity of the proteasome (W. Hilt and D. H. Wolf, personal communication). Thus, the centers of PGPH and tryptic activity seem to be in close spatial relationship, a finding that is in accordance with our model of subunit arrangement in the β-rings.

Determination of the crystal structure of the *Thermoplasma* proteasome has shown that each β subunit not only contains the active site consisting of Thr-1 (together with Lys-33 and Glu-17) but also a hydrophobic pocket that seems to be a substrate binding pocket since it binds the aldehyde inhibitor Ac-Leu-Leu-norleucinal (6). Nevertheless, single β subunits are proteolytically inactive and have to cooperate with adjacent β subunits to exert proteolytic activity (18). In the human proteasome these "cooperating" subunits may be $C7_I$, N3, and C5 or $C10_{II}$ in the centers for chymotryptic, PGPH, and tryptic activities, respectively. Since at least two additional activities, namely the branched chain amino acid preferring activity and the small neutral amino acid preferring activity, have been found in mammalian proteasomes (8), it is likely that the three "cooperating" subunits as well as subunit $C10_{II}$ are actually involved in forming these active sites.

Mammalian proteasomes are able to cut out oligopeptides from proteins that are then presented by major histocompatibility complex class I molecules (39–41). These peptides, which usually consist of 8–9 amino acids, are thought to be produced by simultaneous cleavages (42). A prerequisite for this to happen would be that the distance between two active sites corresponds to the length of an octa- or nonapeptide. This has been shown to be the case in the *Thermoplasma* proteasome (6). Our model of the human proteasome contains only delta and Z as neigboring active β subunits, while in this respect MB1 is in an isolated position and not directly adjacent to another active β subunit. However, hydrophobic amino acids are preferred C termini of antigenic peptides presented by major histocompatibility complex class I (43) and are likely to be produced at the active site of subunit MB1. Therefore, as suggested above, one of the direct neighboring subunits of MB1 may be involved in production of antigenic peptides with hydrophobic C termini according to the molecular ruler mechanism.

α Subunits form not only the framework for correct assembly of β subunits during biogenesis of the 20S proteasome, but they may also affect the proteolytic activities of the 20S proteasome as gene disruption of Y13, the yeast homologue of the α subunit C9, results in a persisting chymotryptic activity that cannot further be stimulated by SDS as can wild-type proteasomes (44). In harmony with this observation C9 is neighbor to MB1, which is involved in the chymotryptic activity. In addition, α subunits also contain information for binding of regulatory complexes such as PA700 and PA28 (20). A motif proposed to be involved in protein–protein interaction is the KEKE sequence (45) present in subunits C9 and XAPC7, which are direct neighbors and thus may form a center for association of PA700. The orientation of two PA700 activator complexes bound to the terminal α-rings of the 20S protea-

some clearly reflects the 2-fold symmetry (46). This implies an alignment of the activator along the diameter approximately vertical to the 2-fold axis of the 20S proteasome—i.e., along a line from C2 to C3/C9. The functional implication of such an arrangement for substrate recognition, unfolding, and transport into the 20S proteasome are subjects for future investigations.

We cannot exclude the possibility that the subunit arrangement could differ in proteasomes from other sources, or in proteasomes containing the interferon-inducible subunits LMP2, LMP7, and MECL1. The model of the subunit arrangement within the α- and β-rings of the human 20S proteasome, as it results from our combined chemical and microscopic experiments, constitutes a first step in solving the quaternary structure of the human proteasome. Resolution of the quaternary structure at the level of molecular interactions of the different subunits remains to be solved by x-ray crystallographic analysis.

We thank Dr. L. Kuehn to support us with some purified proteasome. This work was partially funded by the Danish Natural Science Research Council, by the Deutsche Forschungsgemeinschaft, by the Ministerium für Wissenschaft und Forschung des Landes Nordrhein-Westfalen (Düsseldorf), and by the Bundesministerium für Gesundheit (Bonn). Our collaboration was also supported by a North Atlantic Treaty Organization grant.

1. Hilt, W. & Wolf D. H. (1996) *Trends Biochem. Sci.* **21,** 96–102.
2. Coux, O. Tanaka, K. & Goldberg, A. L. (1996) *Annu. Rev. Biochem.* **65,** 801–847.
3. Groettrup, M., Soza, A., Kuckelkorn, U. & Kloetzel, P. M. (1996) *Immunol. Today* **17,** 429–435.
4. Grizwa, A. Baumeister, W. Dahlmann, B. & Kopp, F. (1991) *FEBS Lett.* **290,** 186–190.
5. Pühler, G., Weinkauf, S., Bachmann, L., Müller, S., Engel, A., Hegerl, R. & Baumeister, W. (1995) *EMBO J.* **11,** 1607–1616.
6. Löwe, J., Stock, D., Jap, B., Zwickl, P., Baumeister, W. & Huber, R. (1995) *Science* **268,** 533–539.
7. Seemüller, E., Lupas, V., Stock, D., Löwe, J., Huber, R. & Baumeister, W. (1995) *Science* **268,** 579–582.
8. Orlowski, M., Cardozo, L. & Michaud, C. (1993) *Biochemistry* **32,** 1563–1572.
9. Heinemeyer, W., Tröndle, N., Albrecht, G. & Wolf, D. H. (1994) *Biochemistry* **33,** 12229–12237.
10. Heinemeyer, W., Kleinschmidt, J. A., Saidowsky, J., Escher, C. & Wolf, D. H. (1991) *EMBO J.* **10,** 555–562.
11. Heinemeyer, W., Gruhler, A., Möhrle, V., Mahé, Y. & Wolf, D. H. (1993) *J. Biol. Chem.* **268,** 5115–5120.
12. Enenkel, C., Lehmann, H., Kipper, J., Guckel, R., Hilt, W. & Wolf, D. H. (1994) *FEBS Lett.* **341,** 193–196.
13. Hilt, W., Enenkel, C., Gruhler, A., Singer, T., Wolf, D. H. (1993) *J. Biol. Chem.* **268,** 3479–3486.
14. Akiyama, K., Yokota, K., Kagawa, S., Shimbara, N., Tamura, T., Akioka, H., Nothwang, H. G., Noda, C., Tanaka, K. & Ichihara, H. (1994) *Science* **265,** 1231–1234.
15. Belich, M. P., Glynne, R. J., Senger, G., Sheer, D. & Trowsdale, J. (1994) *Curr. Biol.* **4,** 769–776.
16. Groettrup, M., Kraft, R., Kostka, S. Standers, S., Stohwasser, R. & Kloetzel, P. M. (1996) *Eur. J. Immunol.* **26,** 863–869.
17. Hisamatasu, H., Shimbara, N., Saito, Y., Kristensen, P., Hendil, K. B., Fujiwara, T., Takahashi, E., Tanahashi, N., Tamura, T., Ichihara, A. & Tanaka, K. (1996) *J. Exp. Med.* **183,** 1807–1816.
18. Zwickl, P., Kleinz, J. & Baumeister, W. (1994) *Nat. Struct. Biol.* **1,** 765–770.
19. Frentzel, S., Pesold-Hurt, B., Seelig, A. & Kloetzel, P. M. (1994) *J. Mol. Biol.* **236,** 975–981.
20. Hoffman, L. & Rechsteiner, M. (1996) *Curr. Top. Cell. Reg.* **34,** 1–32.
21. Kopp, F., Dahlmann, B. & Hendil, K. B. (1993) *J. Mol. Biol.* **229,** 14–19.
22. Hendil, K. B., Kristensen, P. & Uerkvitz, W. (1995) *Biochem. J.* **305,** 245–252.
23. Kristensen, P., Johnson, A. H., Uerkvitz, W., Tanaka, K. & Hendil, K. B. (1994) *Biochem. Biophys. Res. Commun.* **205,** 1785–1789.
24. Lachmann, P. I., Strangeways, L., Vyakarnam, A. & Evan G. (1986) in *Synthetic Peptides as Antigens*, Ciba Foundation Symposium 119, eds. Porter, R. & Whelan, Y. (Wiley, Chichester, U.K.), pp. 25–40.
25. Lomant, A. J. & Fairbanks, G. (1976) *J. Mol. Biol.* **104,** 243–261.
26. Ji, T. H. (1983) *Biochim. Biophys. Acta* **559,** 39–69.
27. Walleczek, J., Martin, T., Redl, B., Stöffler-Meilicke, M. & Stöffler, G. (1989) *Biochemistry* **28,** 4099–4105.
28. Laemmli, U. K. (1970) *Nature (London)* **227,** 680–685.
29. Kurth, J. & Stoffel, W. (1990) *Biol. Chem. Hoppe-Seyler* **371,** 675–683.
30. O'Farrell, P. H. (1975) *J. Biol. Chem.* **250,** 4007–4021.
31. Kopp, F., Kristensen, P., Hendil, K. B., Johnson, A., Sobek, A. & Dahlmann, B. (1995) *J. Mol. Biol.* **248,** 264–272.
32. Schauer, T. M., Nesper, M., Kehl, M., Lottspeich, F., Müller-Taubenberger, A., Gerisch, G. & Baumeister, W. (1993) *J. Struct. Biol.* **111,** 135–147.
33. Chen, P. & Hochstrasser, M. (1996) *Cell* **86,** 961–972.
34. Akiyama, K., Kagawa, S., Tamura, T., Shimbara, N., Takashina, M., Kristensen, P., Hendil, K. B., Tanaka, K. & Ichihara, A. (1994) *FEBS Lett.* **343,** 85–88.
35. Tanaka, K. (1995) *Mol. Biol. Rep.* **21,** 21–26.
36. Nishimura, C., Tamura, T., Tokunaga, F., Tanaka, K. & Ichihara, A. (1993) *FEBS Lett.* **332,** 52–56.
37. Nothwang, H. G., Tamura, T., Tanaka, K. & Ichihara, A. (1994) *Biochim. Biophys. Acta* **1219,** 361–368.
38. Gerards, W. L. H., Hop, F. W. H., Hendriks, I. L. A. M. & Bloemendal, H. (1994) *FEBS Lett.* **346,** 151–155.
39. Boes, B., Hengel, H., Ruppert, T., Multhaupt, G., Koszinowski, U. H. & Kloetzel, P. M. (1994) *J. Exp. Med.* **179,** 901–909.
40. Dick, L. D., Aldrich, C., Jameson, S. C., Moomaw, C. R., Pramanik, B. C., Doyle, C. K., DeMartino, G. N., Bevan, M. J., Forman, J. M. & Slaughter, C. A. (1994) *J. Immunol.* **152,** 3884–3894.
41. Rock, K. L., Gramen, C., Rothstein, L., Clark, K., Sein, R., Dick, L., Hwang, D. & Goldberg, A. L. (1994) *Cell* **78,** 761–771.
42. Dick, T. P., Ruppert, T., Groettrup, M., Kloetzel, P. M., Kuehn, L., Koszinowski, U. H., Stevanovic, S., Schild, H. & Rammensee, H. G. (1996) *Cell* **86,** 253–262.
43. Elliot, T., Smith, M., Driscoll, P. & McMichael, A. (1993) *Curr. Biol.* **3,** 854–866.
44. Emori, Y., Tsukahara, T., Kawasaki, H., Ishiura, S., Sugita, H. & Suzuki, K. (1991) *Mol. Cell. Biol.* **11,** 344–353.
45. Realini, C., Rogers, S. W. & Rechsteiner, M. (1994) *FEBS Lett.* **348,** 109–113.
46. Peters, J. M., Cejka, Z., Harris, J. R., Kleinschmidt, J. A. & Baumeister, W. (1993) *J. Mol. Biol.* **234,** 932–937.
47. Fenteany, G., Standaert, R. F., Lane, W. S., Choi, S., Corey, E. J. & Schreiber, S. L. (1995) *Science* **268,** 726–731.